

Revealing di-pion correlations for the observed substructure near the $\pi^+\pi^-$ mass threshold in $\psi(3686) \rightarrow J/\psi\pi^+\pi^-$

Zhong-Yu Wang^{1,*}, Zhe Liu^{2,3,4,6,†} and Xiang Liu^{2,3,4,5,6,‡}

¹College of Physics, Guizhou University, Guiyang 550025, China

²School of Physical Science and Technology, Lanzhou University, Lanzhou 730000, China

³Lanzhou Center for Theoretical Physics, Key Laboratory of Theoretical Physics of Gansu Province, Lanzhou University, Lanzhou 730000, China

⁴Key Laboratory of Quantum Theory and Applications of MoE, Lanzhou University, Lanzhou 730000, China

⁵MoE Frontiers Science Center for Rare Isotopes, Lanzhou University, Lanzhou 730000, China

⁶Research Center for Hadron and CSR Physics, Lanzhou University and Institute of Modern Physics of CAS, Lanzhou 730000, China

(Dated: November 14, 2025)

Based on the world's largest $\psi(3686)$ data sample, the BESIII Collaboration recently reported a substructure near the $\pi^+\pi^-$ mass threshold in the decay $\psi(3686) \rightarrow J/\psi\pi^+\pi^-$, challenging the established understanding of the di-pion invariant mass spectrum. We propose that this substructure arises directly from di-pion correlations. Using a chiral unitary approach, we successfully reproduce the observed anomaly, thereby providing strong evidence of di-pion correlation in heavy quarkonium decays. This approach also allows us to predict the corresponding di-pion correlation function.

Matter correlations are an interesting and universal phenomenon, spanning from the microscopic to the macroscopic scale. They are a direct result of interactions, and thus, investigating them can reveal how matter interacts. Among these, hadron correlations have received significant attention in recent years [1–16], driven by the accumulation of experimental data. A primary objective of this research is to deepen our understanding of the non-perturbative aspects of the strong interaction, which is a central problem in modern particle physics.

Very recently, the BESIII Collaboration reported a substructure near the $\pi^+\pi^-$ mass threshold in the decay $\psi(3686) \rightarrow J/\psi\pi^+\pi^-$ [17]. Earlier measurements of the di-pion invariant mass spectrum in this decay [18–20] motivated the application of the QCD multipole expansion (QCDME) method, as proposed in Ref. [21], to study low-lying heavy quarkonium transitions. The process $\psi(3686) \rightarrow J/\psi\pi^+\pi^-$ represents a case where the QCDME approach works particularly well [22]. In recent years, the BESIII detector has accumulated the world's largest $\psi(3686)$ data sample, comprising $(2712.4 \pm 1.4) \times 10^6$ events, which enabled the first observation of a substructure near the $\pi^+\pi^-$ mass threshold in this decay channel [17, 23]. This finding highlights the potential of high-precision hadron spectroscopy.

This unexpected observation challenges the established understanding of the di-pion invariant mass spectrum in $\psi(3686) \rightarrow J/\psi\pi^+\pi^-$. We proposed that the observed substructure near the $\pi^+\pi^-$ mass threshold originated directly from di-pion correlations. Using a chiral unitary approach [24–28], we successfully reproduced the substructure, providing strong evidence for di-pion correlations in heavy quarkonium decays.

We present the theoretical formalism for the reaction $\psi(3686) \rightarrow J/\psi\pi^+\pi^-$ via final-state interactions. Given that

both the initial state $\psi(3686)$ and the final state J/ψ have spin $J = 1$, while the π^+ and π^- in the final state have spin $J = 0$, we construct the following decay amplitude structure

$$t = \epsilon_\mu(\psi(3686))\epsilon^{*\mu}(J/\psi)\tilde{t}_{\pi^+\pi^-}, \quad (1)$$

where $\tilde{t}_{\pi^+\pi^-}$ denotes the S -wave transition amplitude for $\pi^+\pi^-$ scattering within coupled channels. In principle, an S -wave interaction exists between J/ψ and π^+ (or π^-), but its contribution to the low-energy region of the $\pi^+\pi^-$ invariant mass distribution is negligible. Moreover, interactions between J/ψ and $\pi^+(\pi^-)$ are suppressed by the Okubo–Zweig–Iizuka (OZI) rule and are therefore disregarded.

To identify the appropriate combination of three mesons in the $\psi(3686)$ decay, we introduce the quark-level flavor-space matrix $M = (q_i\bar{q}_j)$, i.e.,

$$M = \begin{pmatrix} u\bar{u} & u\bar{d} & u\bar{s} & u\bar{c} \\ d\bar{u} & d\bar{d} & d\bar{s} & d\bar{c} \\ s\bar{u} & s\bar{d} & s\bar{s} & s\bar{c} \\ c\bar{u} & c\bar{d} & c\bar{s} & c\bar{c} \end{pmatrix}. \quad (2)$$

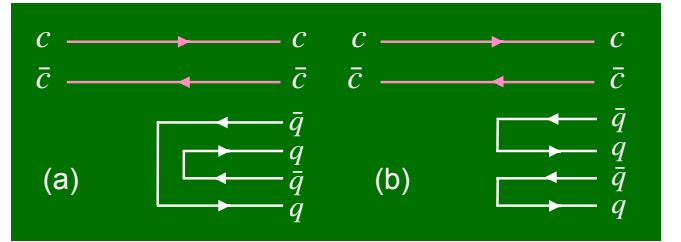


FIG. 1: Topological diagrams corresponding to the (a) $(M)_{44}\text{Tr}(M \cdot M)$ and (b) $(M)_{44}\text{Tr}(M)\text{Tr}(M)$ terms.

The properties of this matrix are detailed in Refs. [29, 30]. For the initial $\psi(3686)$ state, which is composed of a $c\bar{c}$ pair and represented by the $(4, 4)$ element of M , the physically accessible final-state configurations arise from terms such as $(M \cdot M \cdot M)_{44}$, $(M \cdot M)_{44}\text{Tr}(M)$, $(M)_{44}\text{Tr}(M \cdot$

*Electronic address: zhongyuwang@gzu.edu.cn

†Electronic address: zhliu20@lzu.edu.cn

‡Electronic address: xiangliu@lzu.edu.cn

M), and $(M)_{44}\text{Tr}(M)\text{Tr}(M)$. Specifically, for the decay $\psi(3686) \rightarrow J/\psi\pi^+\pi^-$, where final-state interactions are confined to the $\pi\pi$ subsystem and $J/\psi\pi$ interactions are absent, only the last two OZI-suppressed terms— $(M)_{44}\text{Tr}(M \cdot M)$ and $(M)_{44}\text{Tr}(M)\text{Tr}(M)$ —contribute. This contribution arises from replacing the quark-level matrix M in these terms with the pseudoscalar meson matrix P and the vector meson matrix V^μ , yielding $(V^\mu)_{44}\text{Tr}(P \cdot P)$ and $(V^\mu)_{44}\text{Tr}(P)\text{Tr}(P)$. The matrices P and V^μ are defined as:

$$P = \begin{pmatrix} \frac{\eta}{\sqrt{3}} + \frac{\eta'}{\sqrt{6}} + \frac{\pi^0}{\sqrt{2}} & \pi^+ & K^+ & \bar{D}^0 \\ \pi^- & \frac{\eta}{\sqrt{3}} + \frac{\eta'}{\sqrt{6}} - \frac{\pi^0}{\sqrt{2}} & K^0 & D^- \\ K^- & \bar{K}^0 & -\frac{\eta}{\sqrt{3}} + \sqrt{\frac{2}{3}}\eta' & D_s^- \\ D^0 & D^+ & D_s^+ & \eta_c \end{pmatrix}, \quad (3)$$

$$V^\mu = \begin{pmatrix} \frac{\omega+\rho^0}{\sqrt{2}} & \rho^+ & K^{*+} & \bar{D}^{*0} \\ \rho^- & \frac{\omega-\rho^0}{\sqrt{2}} & K^{*0} & D^{*-} \\ K^{*-} & \bar{K}^{*0} & \phi & D_s^{*-} \\ D^{*0} & D^{*+} & D_s^{*+} & J/\psi \end{pmatrix}^\mu. \quad (4)$$

The term $(M)_{44}\text{Tr}(M \cdot M)$ contributes to the process depicted in Fig. 1(a), yielding the following three-meson combination

$$|H^{(1)}\rangle = 2J/\psi\pi^+\pi^- + J/\psi\pi^0\pi^0 + 2J/\psi K^+K^- + 2J/\psi K^0\bar{K}^0 + J/\psi\eta\eta. \quad (5)$$

The term $(M)_{44}\text{Tr}(M)\text{Tr}(M)$ contributes to the process in Fig. 1(b), giving

$$|H^{(2)}\rangle = \frac{1}{3}J/\psi\eta\eta. \quad (6)$$

For Eq. (5), the decay $\psi(3686) \rightarrow J/\psi\pi^+\pi^-$ proceeds through both tree-level and S -wave pseudoscalar-pseudoscalar interactions, as shown in Fig. 2(a). For Eq. (6), the $\pi^+\pi^-$ pair in the final state originates solely from the $\eta\eta$ channel via final-state interactions during the initial production stage. Figure 2(b) illustrates the corresponding rescattering contributions.

The total amplitude is expressed as

$$\begin{aligned} \tilde{t}_{\pi^+\pi^-}(M_{23}) = & V_1 [2 + 2G_{\pi^+\pi^-}(M_{23})T_{\pi^+\pi^- \rightarrow \pi^+\pi^-}(M_{23}) \\ & + \sqrt{2}G_{\pi^0\pi^0}(M_{23})T_{\pi^0\pi^0 \rightarrow \pi^+\pi^-}(M_{23}) \\ & + 2G_{K^+K^-}(M_{23})T_{K^+K^- \rightarrow \pi^+\pi^-}(M_{23}) \\ & + 2G_{K^0\bar{K}^0}(M_{23})T_{K^0\bar{K}^0 \rightarrow \pi^+\pi^-}(M_{23}) \\ & + \sqrt{2}G_{\eta\eta}(M_{23})T_{\eta\eta \rightarrow \pi^+\pi^-}(M_{23})] \\ & + \frac{\sqrt{2}}{3}V_2 e^{i\phi} G_{\eta\eta}(M_{23})T_{\eta\eta \rightarrow \pi^+\pi^-}(M_{23}), \end{aligned} \quad (7)$$

where V_1 and V_2 are the decay strengths from Eqs. (5) and (6), respectively. A relative phase ϕ is introduced between these two decay mechanisms. We treat these parameters as constants and determine their values by fitting to the BESIII experimental data. Here, M_{ij} denotes the invariant mass of a meson pair, with subscripts 12, 13, and 23 corresponding to the final-state particle pairs $J/\psi\pi^+$, $J/\psi\pi^-$, and $\pi^+\pi^-$, respectively.

A factor of 2 arises in identical-particle channels $\pi^0\pi^0$ and $\eta\eta$, canceling the 1/2 factor in their loop function. The additional factor of $\sqrt{2}$ in these channels stems from the unitary normalization used in the chiral unitary approach: $|\pi^0\pi^0\rangle \rightarrow \frac{1}{\sqrt{2}}|\pi^0\pi^0\rangle$ and $|\eta\eta\rangle \rightarrow \frac{1}{\sqrt{2}}|\eta\eta\rangle$. For further discussion, see Refs. [24, 31].

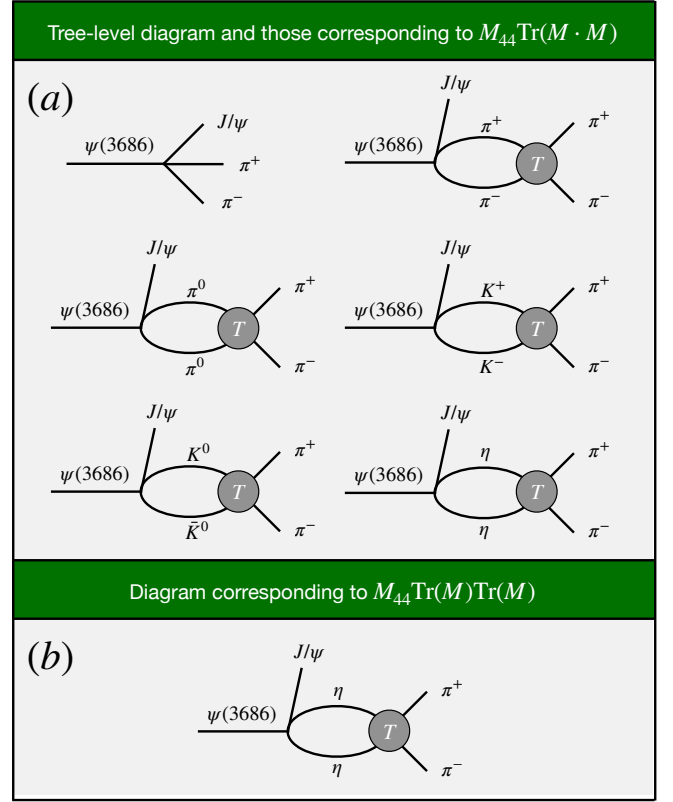


FIG. 2: Diagrams contributing to $\psi(3686) \rightarrow J/\psi\pi^+\pi^-$.

The loop function G for two mesons is expressed using the three-momentum cutoff formulation from Ref. [24]

$$G_{ii}(s) = \int_0^{q_{\max}} \frac{q^2 dq}{(2\pi)^2} \frac{\omega_1 + \omega_2}{\omega_1 \omega_2 [s - (\omega_1 + \omega_2)^2 + i\epsilon]}, \quad (8)$$

where $\omega_i(\vec{q}) = \sqrt{\vec{q}^2 + m_i^2}$, with m_1 and m_2 being the masses of the two mesons in the coupled channels, and q_{\max} is a free parameter. The loop function in dimensional regularization is given by [28, 32–35]

$$\begin{aligned} G_{ii}(s) = & \frac{1}{16\pi^2} \left\{ a_i(\mu) + \ln \frac{m_1^2}{\mu^2} + \frac{m_2^2 - m_1^2 + s}{2s} \ln \frac{m_2^2}{m_1^2} \right. \\ & + \frac{q_{cmi}(s)}{\sqrt{s}} \left[\ln(s - (m_2^2 - m_1^2) + 2q_{cmi}(s)\sqrt{s}) \right. \\ & + \ln(s + (m_2^2 - m_1^2) + 2q_{cmi}(s)\sqrt{s}) \\ & - \ln(-s - (m_2^2 - m_1^2) + 2q_{cmi}(s)\sqrt{s}) \\ & \left. \left. - \ln(-s + (m_2^2 - m_1^2) + 2q_{cmi}(s)\sqrt{s}) \right] \right\}, \end{aligned} \quad (9)$$

where μ is the renormalization scale, $a_i(\mu)$ is the subtraction constant, and $q_{\text{cmi}}(s)$ is the center-of-mass momentum

$$q_{\text{cmi}}(s) = \frac{\lambda^{1/2}(s, m_1^2, m_2^2)}{2\sqrt{s}} \quad (10)$$

with $\lambda(a, b, c) = a^2 + b^2 + c^2 - 2(ab + ac + bc)$.

Due to singularities in the three-momentum cutoff scheme above threshold, we adopt dimensional regularization. To minimize free parameters, the subtraction constant $a_i(\mu)$ is determined by matching the loop functions of both schemes at the threshold of a given channel, as in Refs. [36–40]

$$a_i(\mu) = 16\pi^2 [G^{\text{CO}}(s_{\text{thr}}, q_{\text{max}}) - G^{\text{DR}}(s_{\text{thr}}, \mu)], \quad (11)$$

where G^{CO} and G^{DR} are defined by Eqs. (8) and (9), respectively. We set $q_{\text{max}} = \mu = 0.6$ GeV, determined by fitting to experimental data for the $f_0(500)$ and $f_0(980)$ states; this value is widely used in subsequent theoretical works.

We consider coupled-channel interactions for isospin $I = 0$, including five channels: $\pi^+\pi^-$, $\pi^0\pi^0$, K^+K^- , $K^0\bar{K}^0$, and $\eta\eta$. The transition amplitude $T_{i \rightarrow \pi^+\pi^-}$ in Eq. (7) is obtained by solving the on-shell Bethe–Salpeter equation [24–26, 41]

$$T = [1 - VG]^{-1}V, \quad (12)$$

where V represents the S -wave interaction for $\pi^+\pi^-$ with its coupled channels, derived from the chiral effective Lagrangian. Explicit forms are given in Refs. [29, 42]:

$$\begin{aligned} V_{11} &= -\frac{1}{2f^2}s, & V_{12} &= -\frac{1}{\sqrt{2}f^2}(s - m_\pi^2), & V_{13} &= -\frac{1}{4f^2}s, \\ V_{14} &= -\frac{1}{4f^2}s, & V_{15} &= -\frac{1}{3\sqrt{2}f^2}m_\pi^2, & V_{22} &= -\frac{1}{2f^2}m_\pi^2, \\ V_{23} &= -\frac{1}{4\sqrt{2}f^2}s, & V_{24} &= -\frac{1}{4\sqrt{2}f^2}s, & V_{25} &= -\frac{1}{6f^2}m_\pi^2, \\ V_{33} &= -\frac{1}{2f^2}s, & V_{34} &= -\frac{1}{4f^2}s, \\ V_{35} &= -\frac{1}{12\sqrt{2}f^2}(9s - 6m_\eta^2 - 2m_\pi^2), & V_{44} &= -\frac{1}{2f^2}s, \\ V_{45} &= -\frac{1}{12\sqrt{2}f^2}(9s - 6m_\eta^2 - 2m_\pi^2), \\ V_{55} &= -\frac{1}{18f^2}(16m_K^2 - 7m_\pi^2), \end{aligned} \quad (13)$$

where $f = 0.093$ GeV is the pion decay constant.

Finally, the double differential width for the three-body decay is given by [43]

$$\frac{d^2\Gamma}{dM_{12}dM_{23}} = \frac{1}{(2\pi)^3} \frac{1}{8m_{\psi(3686)}^3} M_{12}M_{23} \sum \sum |t|^2, \quad (14)$$

and $d\Gamma/dM_{12}$ and $d\Gamma/dM_{23}$ are obtained by integrating over the other invariant mass variable. The distribution $d\Gamma/dM_{13}$ can be derived using the constraint

$$M_{12}^2 + M_{13}^2 + M_{23}^2 = m_{\psi(3686)}^2 + m_{J/\psi}^2 + m_{\pi^+}^2 + m_{\pi^-}^2. \quad (15)$$

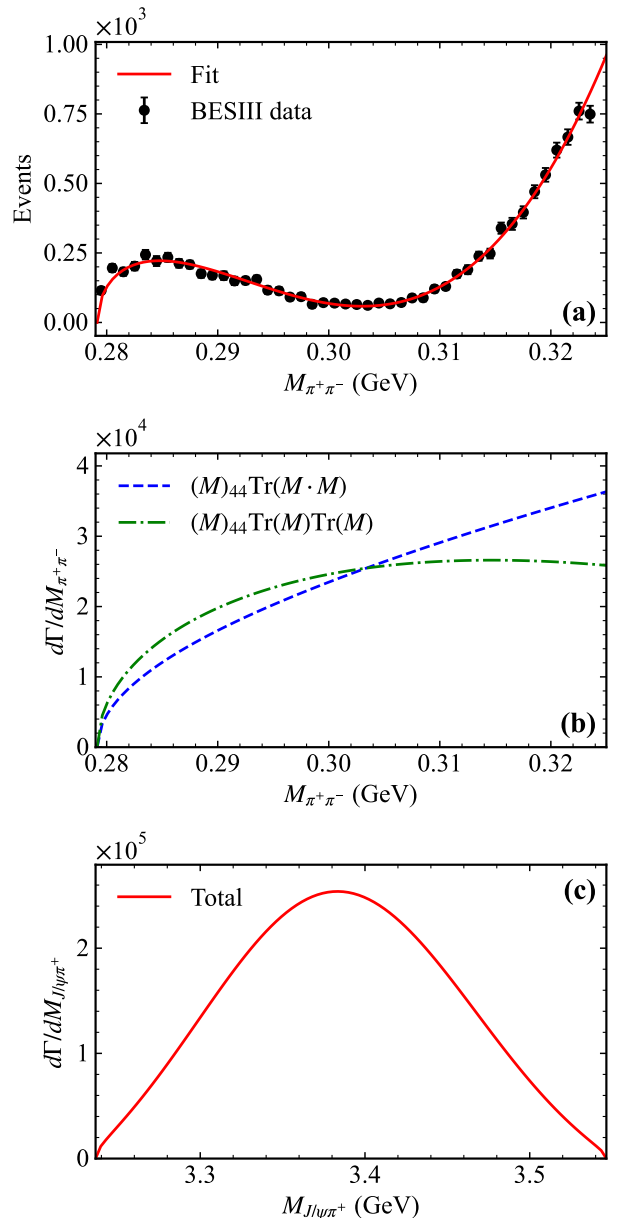


FIG. 3: (a) $\pi^+\pi^-$ invariant mass distribution near threshold in $\psi(3686) \rightarrow J/\psi\pi^+\pi^-$ compared with experimental data [17]. (b) Contributions from the two mechanisms in Fig. 1. (c) $J/\psi\pi^+$ invariant mass spectrum.

We begin by performing a fit to the BESIII experimental data. A new structure located near the $\pi^+\pi^-$ threshold has been reported in the $\pi^+\pi^-$ invariant mass distribution of the decay $\psi(3686) \rightarrow J/\psi\pi^+\pi^-$ [17]. Accordingly, we fit the data in the low-energy region of the $\pi^+\pi^-$ invariant mass distribution, specifically in the range of 0.28–0.32 GeV.

Our theoretical model contains three free parameters: V_1 and V_2 , which denote the strengths of the decay mechanisms shown in Fig. 1, respectively (incorporating an overall normalization factor to match the data), and a relative phase ϕ between them. The fitted values of these parameters are listed

in Table I, yielding $\chi^2/\text{d.o.f.} = 42.86/(45 - 3) = 1.02$.

TABLE I: The theoretical parameters obtained from the fit in the $\psi(3686)$ decay.

Parameters	$V_1 (\times 10^4)$	$V_2 (\times 10^9)$	ϕ (rad)
Fit values	4.23 ± 0.04	1.09 ± 0.01	0.048 ± 0.001

Using the fitted parameters, we compute the $\pi^+\pi^-$ invariant mass distribution, as shown in Fig. 3(a). The black points with error bars represent the BESIII experimental data, and the red solid line corresponds to our fit results. Excellent agreement is observed between theory and experiment. A clear peak is seen around 0.285 GeV in the $\pi^+\pi^-$ spectrum, which drops to a minimum near 0.305 GeV. In our model, this structure does not correspond to a genuine resonance, but results from the interference and superposition of the two decay mechanisms illustrated in Fig. 1. The individual contributions of these two components are displayed in Fig. 3(b). Neither shows any structure in this energy region, and both are of comparable magnitude. Above 0.32 GeV, both the data and the theoretical curve rise steadily, dynamically generated from meson-meson interactions. Moreover, we show the $J/\psi\pi^+$ invariant mass distribution in Fig. 3(c). No resonant structures are observed. The $J/\psi\pi^-$ distribution is identical due to charge symmetry.

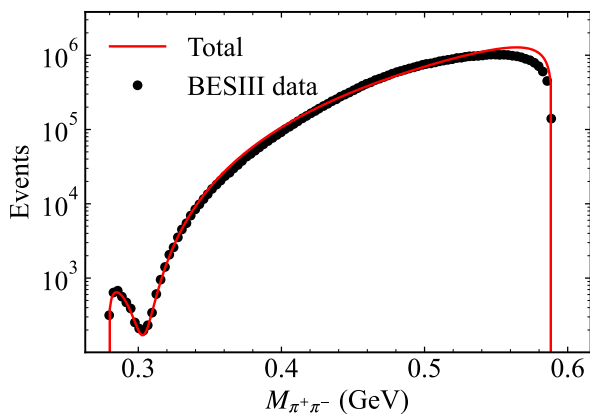


FIG. 4: Full $\pi^+\pi^-$ invariant mass distribution in $\psi(3686) \rightarrow J/\psi\pi^+\pi^-$. Data points are from BESIII [17].

We further show the full $\pi^+\pi^-$ invariant mass spectrum in Fig. 4. Here, no additional fit was performed; we simply applied the parameters from Table I, adjusting only an overall normalization constant to account for the different event statistics between Fig. 3(a) and Fig. 4. This constant affects only the absolute scale, not the spectral shape. The theoretical result agrees well with the experimental data over the full range, with only minor deviations localized around 0.6 GeV. It should be noted that the BESIII data in this region are provided without uncertainties, and the data density is significantly higher than in the low-energy region. For these reasons, we deliberately refrain from fitting the data in Fig. 4. The successful description of the full spectrum using parameters

determined from a local fit to the low-energy region demonstrates the robustness and predictive power of our model.

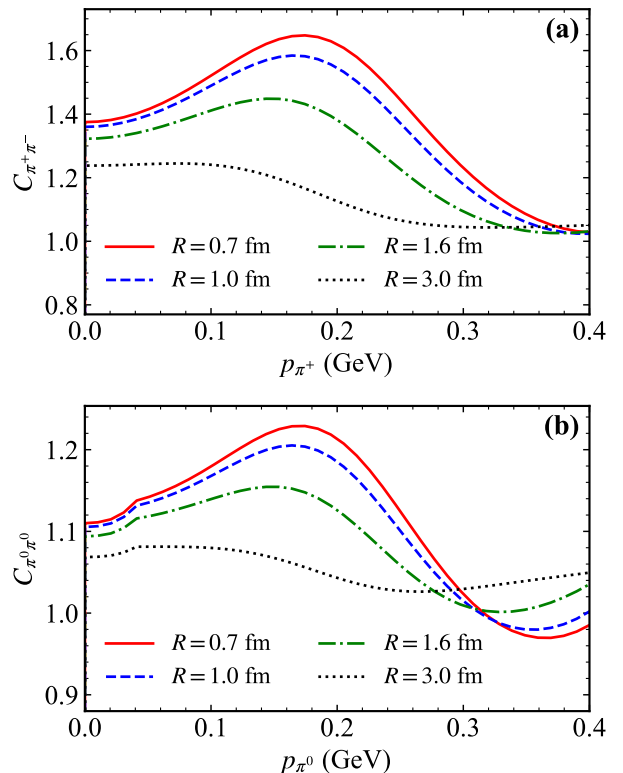


FIG. 5: Source size dependence of the correlation functions with the Gaussian source for $\pi^+\pi^-$ (a) and $\pi^0\pi^0$ (b) in coupled channels, taking $q_{max} = 0.6$ GeV. The results obtained with source sizes $R = 0.7, 1.0, 1.6,$ and 3.0 fm are denoted by the red solid line, the blue dashed line, the green dash-dotted line, and the black dotted line, respectively.

Within this framework, the di-pion correlation function can also be derived. The coupled-channel correlation functions for both charged and neutral pion pairs are expressed as [44–47]

$$\begin{aligned}
 C(p_{\pi^+}) = & 1 + 4\pi\theta(q_{max} - p_{\pi^+}) \int_0^\infty dr r^2 S_{12}(r) \left[|j_0(p_{\pi^+} r)| \right. \\
 & + |T_{\pi^+\pi^- \rightarrow \pi^+\pi^-}(s) \tilde{G}_{\pi^+\pi^-}(r, s)|^2 \\
 & + |\sqrt{2} T_{\pi^0\pi^0 \rightarrow \pi^+\pi^-}(s) \tilde{G}_{\pi^0\pi^0}(r, s)|^2 \\
 & + |T_{K^+K^- \rightarrow \pi^+\pi^-}(s) \tilde{G}_{K^+K^-}(r, s)|^2 \\
 & + |T_{K^0\bar{K}^0 \rightarrow \pi^+\pi^-}(s) \tilde{G}_{K^0\bar{K}^0}(r, s)|^2 \\
 & \left. + |\sqrt{2} T_{\eta\eta \rightarrow \pi^+\pi^-}(s) \tilde{G}_{\eta\eta}(r, s)|^2 - j_0^2(p_{\pi^+} r) \right], \quad (16)
 \end{aligned}$$

and

$$\begin{aligned}
C(p_{\pi^0}) = & 1 + 4\pi\theta(q_{max} - p_{\pi^0}) \int_0^\infty dr r^2 S_{12}(r) \left[|j_0(p_{\pi^0} r) \right. \\
& + \sqrt{2} T_{\pi^0\pi^0 \rightarrow \pi^0\pi^0}(s) \tilde{G}_{\pi^0\pi^0}(r, s) |^2 \\
& + |T_{\pi^+\pi^- \rightarrow \pi^0\pi^0}(s) \tilde{G}_{\pi^+\pi^-}(r, s) |^2 \\
& + |T_{K^+K^- \rightarrow \pi^0\pi^0}(s) \tilde{G}_{K^+K^-}(r, s) |^2 \\
& + |T_{K^0\bar{K}^0 \rightarrow \pi^0\pi^0}(s) \tilde{G}_{K^0\bar{K}^0}(r, s) |^2 \\
& \left. + |\sqrt{2} T_{\eta\eta \rightarrow \pi^0\pi^0}(s) \tilde{G}_{\eta\eta}(r, s) |^2 - j_0^2(p_{\pi^0} r) \right]. \tag{17}
\end{aligned}$$

where the factor of $\sqrt{2}$ necessarily originates from the identical particle symmetrization, as formalized in Eq. (7). Here, the source function is given by

$$S_{12}(r) = \frac{1}{(R\sqrt{4\pi})^3} e^{-\frac{r^2}{4R^2}}, \tag{18}$$

where R represents the size of the source in which the particles are assumed to be produced. Additionally,

$$\tilde{G}_{ii}(r, s) = \int \frac{d^3\vec{q}}{(2\pi)^3} \frac{\omega_1 + \omega_2}{2\omega_1\omega_2} \frac{j_0(\vec{q}r)}{s - (\omega_1 + \omega_2)^2 + i\epsilon}, \tag{19}$$

where $\omega_i(\vec{q})$ defined as in Eq. (8). The scattering matrix elements $T_{i \rightarrow j}$ can be obtained from Eq. (12).

In Eqs. (16)–(17), the source size R dependence of the coupled-channel correlation functions for $\pi^+\pi^-$ and $\pi^0\pi^0$ is shown in Fig. 5(a) and (b), respectively, as a function of the pion momentum. The overall behavior of both results is quite consistent, with each reaching its maximum when the pion momentum is around 0.18 GeV. For $\pi^+\pi^-$ and $\pi^0\pi^0$ pairs, the strength of correlations decreases gradually as the source size R increases. A slight cusp structure is observed in the $\pi^0\pi^0$ correlation, resulting from the $\pi^+\pi^-$ threshold effect. As for the difference between the correlation functions of charged and neutral pions, in addition to the mass difference, the electromagnetic interaction between charged pions also contributes. However, this interaction was not accounted for in

our calculation. The femtoscopy correlation functions in the presence of Coulomb potential have been studied in Ref. [48], which provided a more detailed discussion. These phenomena may be probed experimentally in future studies and could shed light on hadronic interactions.

In summary, the recent discovery of a substructure near the $\pi^+\pi^-$ mass threshold in $\psi(3686) \rightarrow J/\psi\pi^+\pi^-$ by the BESIII Collaboration challenges conventional interpretations of the di-pion invariant mass spectrum. We show that this structure can be explained as a direct manifestation of di-pion correlation. Using a reaction model based on flavor symmetry and a chiral unitary approach to treat di-pion correlation, we successfully reproduce the observed feature, establishing strong evidence of di-pion correlation in heavy quarkonium decays. The measured line shape is shown to stem from the interference between two distinct, yet equally important, OZI-suppressed decay mechanisms. Furthermore, the method enables us to calculate the di-pion correlation function with these fixed parameters. This finding opens a new avenue for studying matter correlations and offers valuable insight into the non-perturbative dynamics of the strong interaction in the low-energy regime.

Acknowledgements

We would like to thank Professor De-Liang Yao for his valuable comments. This work is supported by the Natural Science Special Research Foundation of Guizhou University Grant No. 2024028 and Guizhou Provincial Major Scientific and Technological Program XKBF (2025)010 (Z.Y.W.). This work is also supported by the National Natural Science Foundation of China under Grant Nos. 12335001 and 12247101, the ‘111 Center’ under Grant No. B20063, the Natural Science Foundation of Gansu Province (No. 22JR5RA389, No. 25JRRA799), the Talent Scientific Fund of Lanzhou University, the fundamental Research Funds for the Central Universities (No. lzujbky-2023-stlt01), the project for top-notch innovative talents of Gansu province, and Lanzhou City High-Level Talent Funding.

-
- [1] M. Z. Liu, Y. W. Pan, Z. W. Liu, T. W. Wu, J. X. Lu and L. S. Geng, *Phys. Rept.* **1108**, 1-108 (2025)
- [2] L. Fabbietti, V. Mantovani Sarti and O. Vazquez Doce, *Ann. Rev. Nucl. Part. Sci.* **71**, 377-402 (2021).
- [3] S. Acharya *et al.* [ALICE], *Phys. Lett. B* **822**, 136708 (2021)
- [4] S. Acharya *et al.* [ALICE], *Phys. Rev. Lett.* **127**, no.17, 172301 (2021)
- [5] S. Acharya *et al.* [ALICE], *Phys. Lett. B* **833**, 137335 (2022)
- [6] S. Acharya *et al.* [ALICE], *Phys. Rev. D* **106**, no.5, 052010 (2022)
- [7] S. Acharya *et al.* [ALICE], *Phys. Lett. B* **845**, 138145 (2023)
- [8] S. Acharya *et al.* [ALICE], *Phys. Lett. B* **856**, 138915 (2024)
- [9] S. Acharya *et al.* [ALICE], *Phys. Rev. D* **110**, no.3, 032004 (2024)
- [10] Y. Kamiya, K. Sasaki, T. Fukui, T. Hyodo, K. Morita, K. Ogata, A. Ohnishi and T. Hatsuda, *Phys. Rev. C* **105**, no.1, 014915 (2022)
- [11] Y. Kamiya, T. Hyodo and A. Ohnishi, *Eur. Phys. J. A* **58**, no.7, 131 (2022)
- [12] Z. W. Liu, J. X. Lu and L. S. Geng, *Phys. Rev. D* **107**, no.7, 074019 (2023)
- [13] I. Vidana, A. Feijoo, M. Albaladejo, J. Nieves and E. Oset, *Phys. Lett. B* **846**, 138201 (2023)
- [14] N. Ikeno, G. Toledo and E. Oset, *Phys. Lett. B* **847**, 138281 (2023)
- [15] Y. Yan, Q. Huang, Y. Yang, H. Huang and J. Ping, *Sci. China Phys. Mech. Astron.* **68**, no.3, 232012 (2025)
- [16] S. W. Liu and J. J. Xie, *Phys. Rev. D* **112**, no.3, 034027 (2025)
- [17] M. Ablikim *et al.* [BESIII], [arXiv:2509.23761 [hep-ex]].
- [18] G. S. Abrams, D. Briggs, W. Chinowsky, C. E. Friedberg,

- G. Goldhaber, J. A. Kadyk, A. Litke, B. Lulu, F. Pierre and B. Sadoulet, *et al.* Phys. Rev. Lett. **34**, 1181 (1975)
- [19] T. A. Armstrong *et al.* [Fermilab E760], Phys. Rev. D **55**, 1153-1158 (1997)
- [20] H. Mendez *et al.* [CLEO], Phys. Rev. D **78**, 011102 (2008)
- [21] Y. P. Kuang, Front. Phys. China **1**, 19-37 (2006)
- [22] Y. P. Kuang, J. P. Ma, O. Nachtmann, W. P. Xie and H. H. Zheng, Phys. Rev. D **85**, 114010 (2012)
- [23] M. Ablikim *et al.* [BESIII], Chin. Phys. C **48**, no.9, 093001 (2024)
- [24] J. A. Oller and E. Oset, Nucl. Phys. A **620**, 438-456 (1997) [erratum: Nucl. Phys. A **652**, 407-409 (1999)]
- [25] E. Oset and A. Ramos, Nucl. Phys. A **635**, 99-120 (1998)
- [26] J. A. Oller, E. Oset and J. R. Pelaez, Phys. Rev. Lett. **80**, 3452-3455 (1998)
- [27] J. A. Oller, E. Oset and A. Ramos, Prog. Part. Nucl. Phys. **45**, 157-242 (2000)
- [28] J. A. Oller and U. G. Meissner, Phys. Lett. B **500**, 263-272 (2001)
- [29] W. H. Liang and E. Oset, Phys. Lett. B **737**, 70-74 (2014)
- [30] W. H. Liang, J. J. Xie and E. Oset, Eur. Phys. J. C **76**, no.12, 700 (2016)
- [31] J. M. Dias, F. S. Navarra, M. Nielsen and E. Oset, Phys. Rev. D **94**, no.9, 096002 (2016)
- [32] J. A. Oller and E. Oset, Phys. Rev. D **60**, 074023 (1999)
- [33] D. Gamermann, E. Oset, D. Strottman and M. J. Vicente Vacas, Phys. Rev. D **76**, 074016 (2007)
- [34] L. Alvarez-Ruso, J. A. Oller and J. M. Alarcon, Phys. Rev. D **82**, 094028 (2010)
- [35] Z. H. Guo, L. Liu, U. G. Meißner, J. A. Oller and A. Rusetsky, Phys. Rev. D **95**, no.5, 054004 (2017)
- [36] E. Oset, A. Ramos and C. Bennhold, Phys. Lett. B **527**, 99-105 (2002) [erratum: Phys. Lett. B **530**, 260-260 (2002)]
- [37] G. Montaña, A. Ramos, L. Tolos and J. M. Torres-Rincon, Phys. Rev. D **107**, no.5, 054014 (2023)
- [38] W. Liang, J. Y. Yi, C. W. Xiao and S. Q. Zhou, Phys. Rev. D **108**, no.11, 116001 (2023)
- [39] Z. Y. Wang and W. Liang, Eur. Phys. J. C **85**, no.6, 644 (2025)
- [40] Z. Y. Wang, Y. S. Li and S. Q. Luo, Phys. Rev. D **111**, no.7, 076009 (2025)
- [41] F. K. Guo, P. N. Shen, H. C. Chiang and R. G. Ping, Nucl. Phys. A **761**, 269-282 (2005)
- [42] Z. Y. Wang, J. Y. Yi, Z. F. Sun and C. W. Xiao, Phys. Rev. D **105**, no.1, 016025 (2022)
- [43] S. Navas *et al.* [Particle Data Group], Phys. Rev. D **110**, no.3, 030001 (2024)
- [44] R. Molina, C. W. Xiao, W. H. Liang and E. Oset, Phys. Rev. D **109**, no.5, 054002 (2024)
- [45] R. Molina, Z. W. Liu, L. S. Geng and E. Oset, Eur. Phys. J. C **84**, no.3, 328 (2024)
- [46] H. P. Li, J. Y. Yi, C. W. Xiao, D. L. Yao, W. H. Liang and E. Oset, Chin. Phys. C **48**, no.5, 053107 (2024)
- [47] M. Albaladejo, A. Feijoo, I. Vidaña, J. Nieves and E. Oset, Eur. Phys. J. A **61**, no.8, 187 (2025)
- [48] M. Albaladejo, A. Garcia-Lorenzo and J. Nieves, PTEP **2025**, 09 (2025)